Investigation on in-situ formed Al$_3$V-Al-VC nano composite through conventional, microwave and spark plasma sintering

Ehsan Ghasali [a,b,*], Yasin Orooji [a], Hadi Niknam Germi [c]

[a] College of Materials Science and Engineering, Nanjing Forestry University, No. 159, Longpan Road, Nanjing, 210037 Jiangsu, People's Republic of China
[b] Ceramic Dept, Materials and Energy Research Center, Alborz, Iran
[c] Sahand University of Technology, New Sahand Town, Tabriz, Iran

ARTICLE INFO

ABSTRACT

In the present study, the effect of heating methods has been studied on the microstructure and mechanical properties of in-situ formed Al$_3$V-Al-VC nano-composite. 5 and 15 wt % of VC were added to Al matrix and conventional and microwave sintering processes were performed at 600 °C. While spark plasma sintering process was done at 450 °C with initial and final pressure of 10 and 30 MPa, respectively. The XRD results revealed the formation of Al$_3$V intermetallic compound in microwave sintered sample, while in both spark plasma sintered and conventionally prepared specimens, the only crystalline phases were Al and VC. Microstructure studies, demonstrated a uniform distribution of 5wt% VC reinforcement in Al matrix but the 15wt%VC addition led to form agglomerates in all prepared samples. The highest bending strength (275 ± 13 MPa) and hardness (260 ± 13 Vickers) were obtained in the spark plasma sintered sample with 15wt% of VC content.

1. Introduction

Definitely, the sintering process is one of the most important stages in the preparation of products via powder metallurgy method. Regarding this fact, the sintering temperature acts as an effective parameter in pressureless sintering techniques [1, 2, 3]. It is worth mentioning that the variables of thermal regime in sintering process affect the final properties of the products. Here, the reported or measured temperatures recorded by thermocouples and pyrometers would be considered as the sintering temperature of the sample. On the other hand, each sintering process involves its own generation/transformation mechanism or transfer phenomena between the particles in a micro-scale outlook [4, 5, 6].

In conventional sintering processes, the generated heat transfers to the surfaces and diffuses into the core of the sample through conduction mechanism. This mechanism requires a holding time so that the surface and core temperatures of the sample become equal [7]. Such a simple fact affects the final properties as grain growth, reaction products and so on [8]. On the other hand, microwave sintering combines radiation, conduction and convection mechanisms via susceptors until the sintering target can directly absorb the electromagnetic field. Many of researchers have stated that the heat can be produced by an absorber particle inside the specimens in microwave sintering process [9, 10, 11]. Spark plasma sintering process (SPS) uses pulsed currents to generate heat in the

specimens. Here, the dominating heat transfer mechanism is assumed to be the conduction from mold and also from the sparks between the particles inside the samples. Moreover, this novel process uses Joules heating alongside applied pressure and vacuum condition, that totally affect final properties of the specimen in near-full densification state [12, 13, 14].

Regarding the features of each sintering process, it can be concluded that a change in heating method would change the properties of products as grain size, quality of boundaries, reaction products as a function of local sintering temperature and total sintering time, densification behavior and the bonding of the particles [15, 16, 17].

Metal matrix composites (MMCs) and specially aluminum matrix composites (AMCs) have been interested for the past few decades due to unique advantages such as high specific strength, low density and simple required equipment in a wide range of production [18]. The low melting point of aluminum leads to use economic casting routes and large scale production methods, while the low costs and accessibility of Al powders have made powder metallurgy as an alternative method for preparation of AMCs [19, 20, 21]. To the best of the authors knowledge, numerous ceramic reinforcements have been used to produce AMCs [22, 23, 24], but regarding the detailed investigations, usually most of the reinforcements react with Al and produce intermetallics and interfacial products. In addition to the content and distribution of the
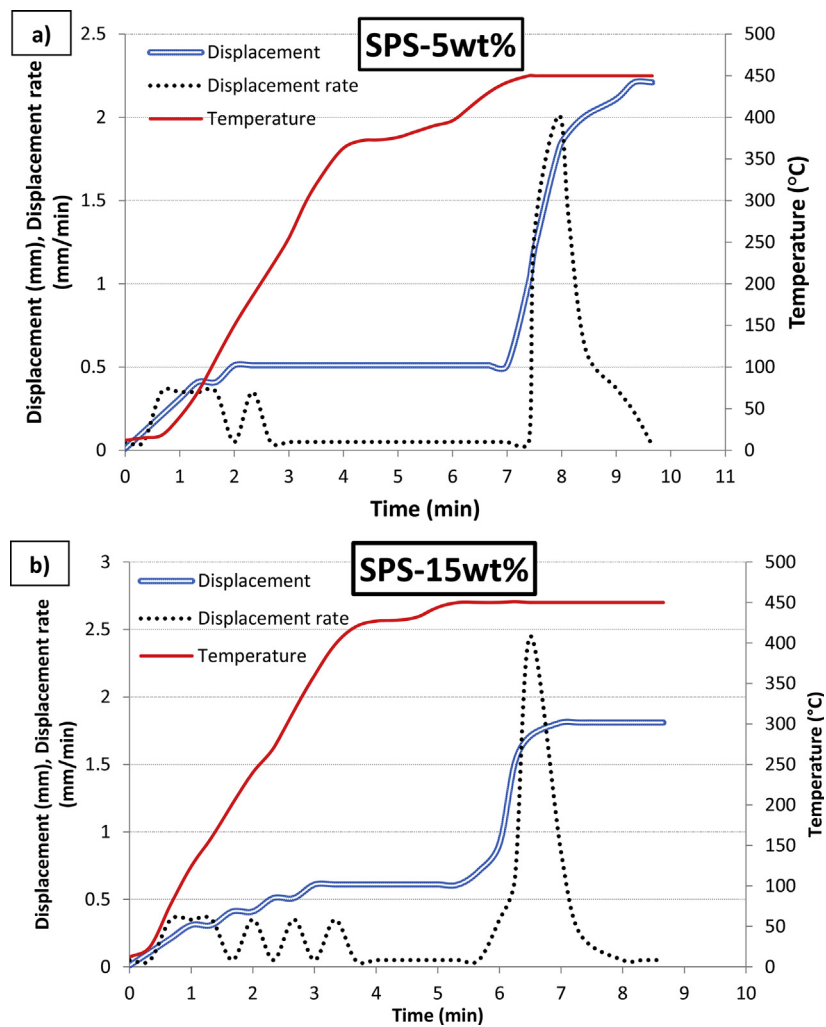

Fig. 1. Displacement, temperature and displacement rate vs. sintering time of SPSed samples: a) Al-5wt%VC and b) Al-15wt%VC.
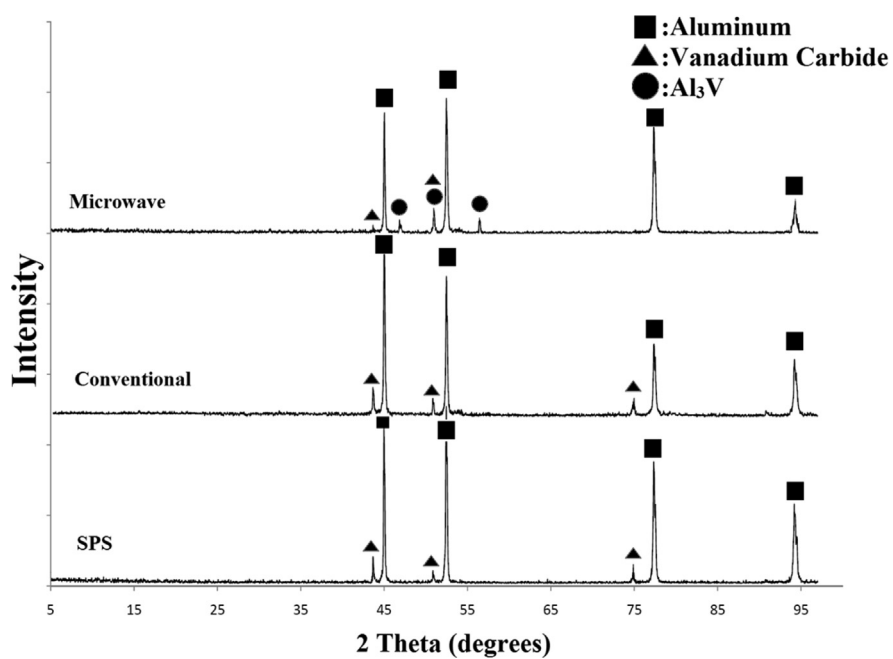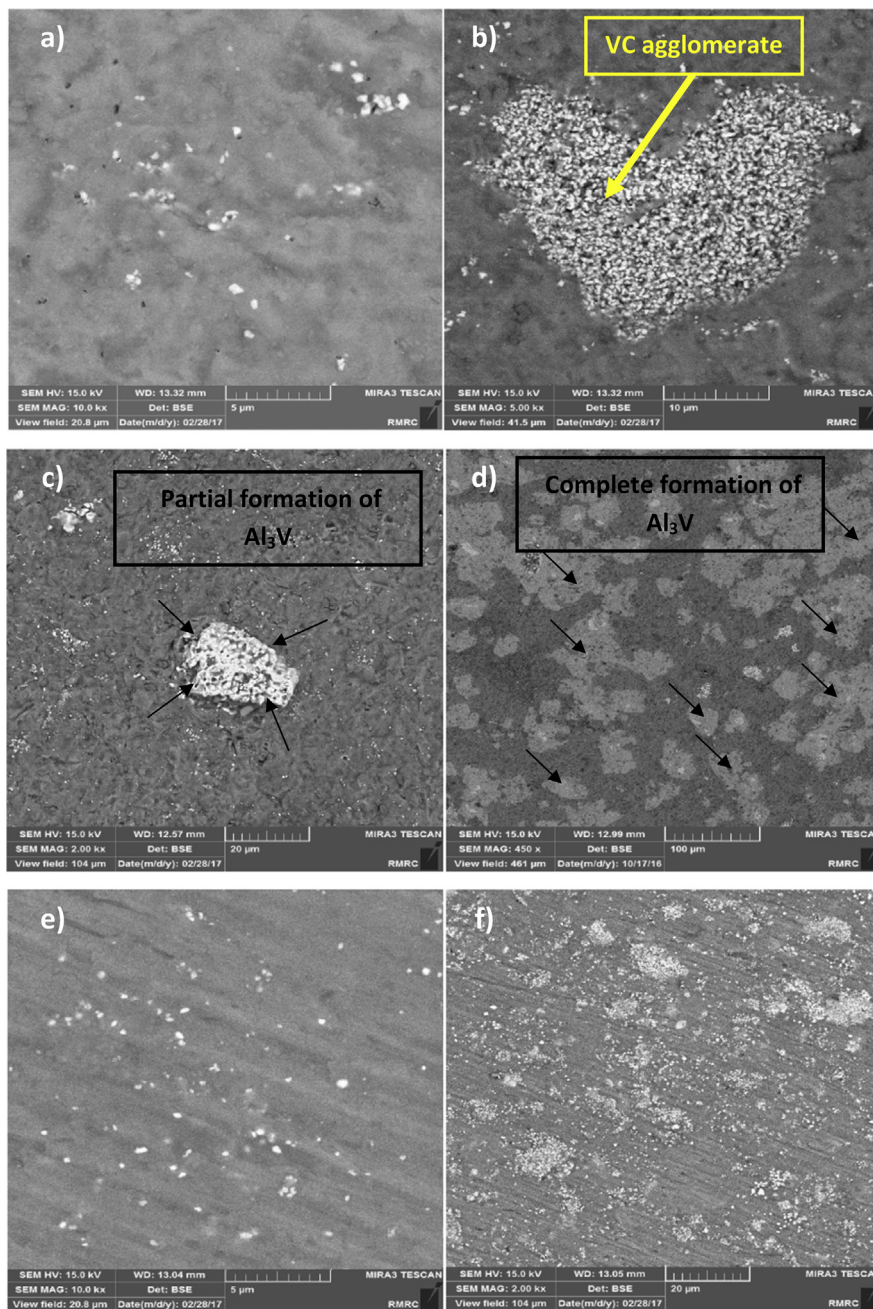

Fig. 2. XRD patterns of Al-15wt%VC composites prepared by spark plasma, microwave and conventional sintering.

Fig. 3. Backscattered FESEM images of Conventionally (a and b), MW (c and d) and SPS (e and f) sintered samples: a,c and e) Al-5wt%VC and b, d and f) Al-15wt%VC nano composites.

reinforcements, reaction products have direct effects on final properties of the samples. These interfacial reactions can be controlled via sintering parameters and somehow the choice of sintering method [25, 26].

Therefore, the present study focuses on the effects of sintering process on phase evaluation, microstructure and mechanical properties of Al-VC nano composites. Moreover, the effects of VC content on formed products at similar sintering temperatures through pressureless (microwave and conventional sintering) and pressure assisted sintering method (SPS) at lower sintering temperatures will be studied.

2. Materials & methods

Aluminum (MERCK Art. no. 1056 aluminum powder, average particle size of 45 μm, 99% purity) and vanadium carbide (average particle size of 100 nm, 99% purity) powders were used as starting materials as reported previously [27]. Two different batches of 5 and 15wt% VC added to aluminum powder in 100 cc of ethanol to obtain a uniform distribution of reinforcement particles in the aluminum matrix by means of a high-energy ball mill. After milling, the mixture was dried at 70 °C on dried at 70 °C using a hot plate after 12 h while stirring. In microwave and conventional sintering processes, the pre-forming was done as uni-axial compression at 250 MPa and bar-shaped samples with 5 × 5 × 25 mm of dimension were prepared, while in SPS the mixed powders were used directly without any pre-pressing process. Conventional sintering was done at 600 °C under a heating rate of 10 °C/min in a graphite bed for 1 h to prevent oxidation. Microwave sintering was performed in an assembled microwave furnace (900 W and 2.45 GHz) at 600 °C without soaking time and protective atmosphere, in a graphite bed as was done in the conventional process. The temperature of microwave furnace was controlled by an optical pyrometer (RAYR312MSCL2G temperature
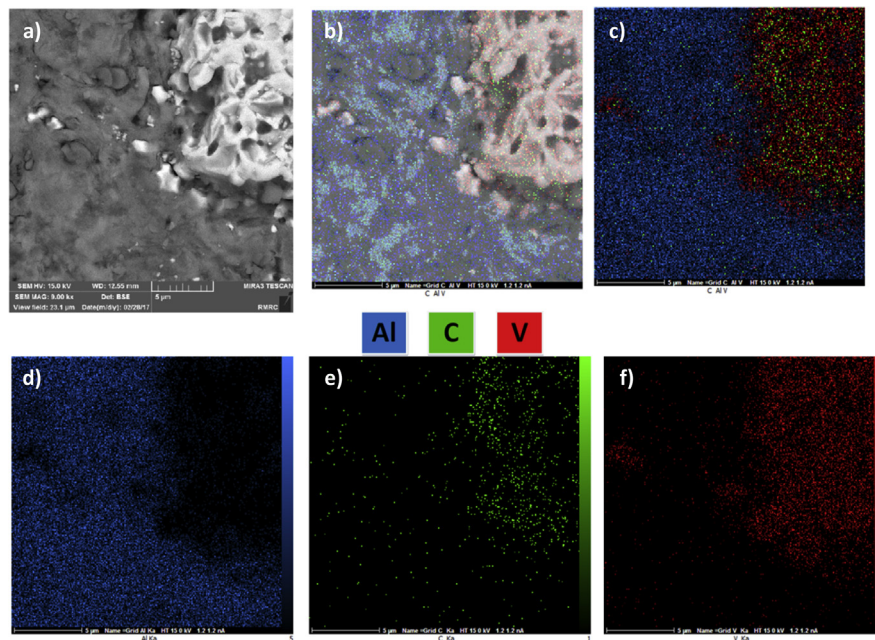
Fig. 4. Backscattered FESEM image of the MW Al-5wt%VC sintered sample at 600 °C (a), overlapping of Al, C and V on original picture as background, overlay of Al, C and V (C) and corresponding EDS elemental mapping of Al (d), C (e) and V(f).

detector). SPS (SPS-20T-10, China) was conducted by inserting the mixed powders directly into a graphite die (30 mm of diameter) and sintering was done at 450 °C under initial and final pressures of 10 MPa (by increasing the temperature) and 30 MPa (at 450 °C), respectively. The temperature in SPS process was determined by placing thermocouple inside the hole at graphite die. Phase identification was carried out via XRD method (Philips X′ Pert System) with a Co k_α ($\lambda = 1.789$ A°) radiation source and an image-plate detector over the 2θ range of 5–100° in reflection geometry. Bulk density of the sintered samples was measured from Archimedes′ principle. Three-point bending flexural test with three pieces was done to examine the strength of the sintered samples. The bending strength test was performed with 18 mm gage length and loading rate of 0.5 mm/min at room temperature. In the case of SPS, sintered samples were cut from the sintering disc with 30 mm of diameter to final size of 5 × 5 × 25 mm according to the same size of prepared samples of microwave and conventional heating [28]. Vickers micro-hardness values of the sintered samples were calculated through at least ten successive indentations for each sample by means of a MKV-h21 Micro-hardness Tester under a load of 1 kgF for 15 s. Microstructural characterization of the sintered samples was performed using FESEM (MIRA 3 TESCAN, Czech Republic) equipped with an energy dispersive spectrometer (EDS). Details of material preparation procedure and the sintering process as well as the microstructural studies are exactly the same as that reported previously [29, 30, 31].

3. Results and discussion

Fig. 1 shows the displacement, temperature and displacement rate vs. sintering time of 5 and 15wt%VC particle-reinforced composites in the SPS process. As can be seen in Fig. 1, SPS sintering of the samples was done at 450 °C in 9–10 minutes. Approximately, two distinguished regions of densification can be realized from Fig. 1: 1) Initial densification at about 0–3.5 min. and, 2) Second stage densification at about 6–9 min. of sintering. The initial densification can be attributed to gas removal and rearrangements of particles that normally occur due to the direct inserting of powder into the mold. The second stage of densification can be related to two possible reasons as the starting sintering phenomena (neck formation and growth) and also increasing the pressure. Moreover,

the comparison between the sintering curves (Fig. 1) demonstrates a higher total displacement for the specimens with 5wt% of VC nano-particles than the Al-15wt%VC composites. Generally, the higher amount of metallic matrix in samples can accelerate the densification due to the occurrence of plastic deformation at elevated temperatures, especially in the case of Al matrix due to the work-softening nature of this element. On the other hand, increasing the ceramic reinforcement contents especially in nano-scale range, can lead to form agglomerates that affect the densification behavior compared to composites containing lower amounts of reinforcements sintered at analogous temperatures.

Fig. 2 reveals the XRD patterns of Al-15wt%VC samples prepared by SPS, MW and conventional sintering. The interfacial reactions between Al and VC in MW process demonstrates the peaks of Al_3V intermetallic compound, while the patterns for SPS and conventionally prepared samples show Al and VC peaks as the only crystalline phases. The thermodynamics agreement and negative Gibbs free energy of Al_3V formation have been reported in the previous work [27], but it is important to mention that the XRD detection range for the interfacial reactions can affect the actual amounts of reaction products. Therefore, the possibilities for the formation of low amounts of Al_3V below the detection range of XRD should be taken into account for the SPS and conventional processes. Also, the reaction between Al and VC has another reaction product as Al_4C_3 which was not detected by XRD patterns. Moreover, the phase identification was carried out using XRD data cards (ICDD: 00-004-0787 (Al), 01-073-0476 (VC), 00-065-2664 (Al_3V)).

Fig. 3 displays the FESEM images of spark plasma, microwave and conventionally-sintered samples. As can be seen in Fig. 3 a and b, conventional heating leads to form agglomerates in the composite containing 15wt%VC, while the sample containing 5wt%VC shows almost a uniform distribution of the reinforcement particles. In the case of microwave sintered samples, the reaction between Al and VC leads to form Al_3V intermetallic compound. Regarding the interfacial reactions, the MW sintered Al-15wt%VC composite shows higher amounts of reaction products compared to the Al-5wt%VC sample. Also, the partial reactions between Al and VC, as can be seen in Fig. 3c and d, confirm the progress of interfacial reactions in comparison to the conventionally-sintered sample at the same sintering temperature (600 °C). The Microstructures of the SPSed samples (Fig. 3 e and f) reveal almost a fine
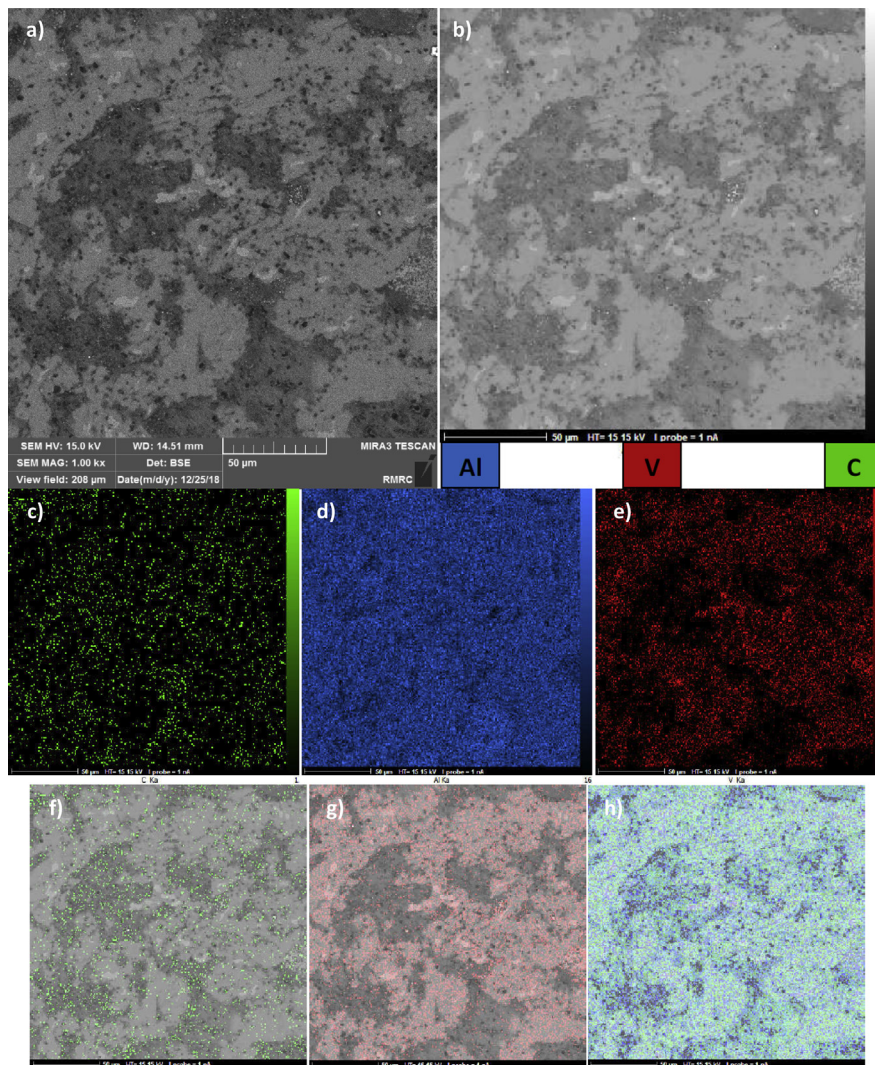
Fig. 5. Backscattered FESEM images of the MW Al-15wt%VC sintered sample at 600 °C (a and b), corresponding EDS elemental mapping of C (c), Al (d) and V(e) and overlapping of C (f), V (g) and Al (h) on original picture as background.
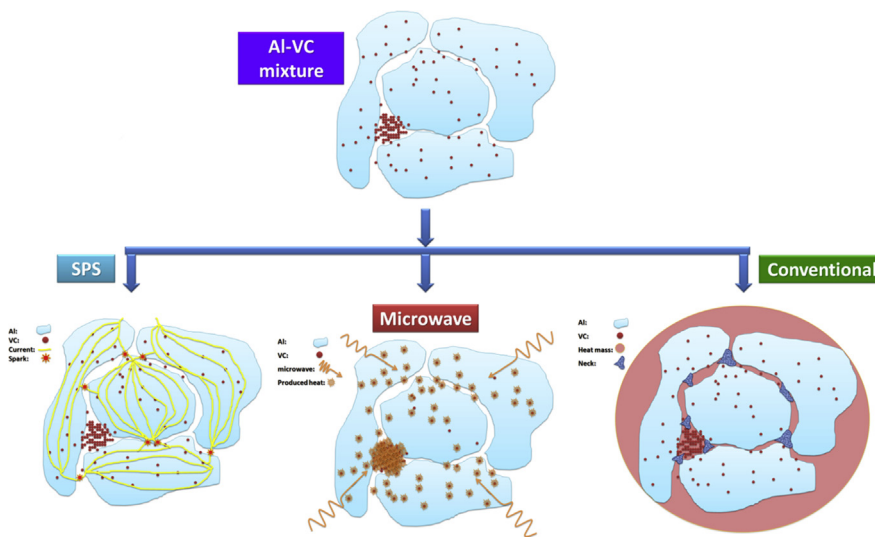

Fig. 6. Schematic principles of different heating methods influence on sintering mechanism.

densification behavior and a uniform distribution of 5wt% VC particles, but in the case of 15wt% VC, the composite shows some formed agglomerates that have more proper dispersions in the matrix than in conventionally-sintered specimen.
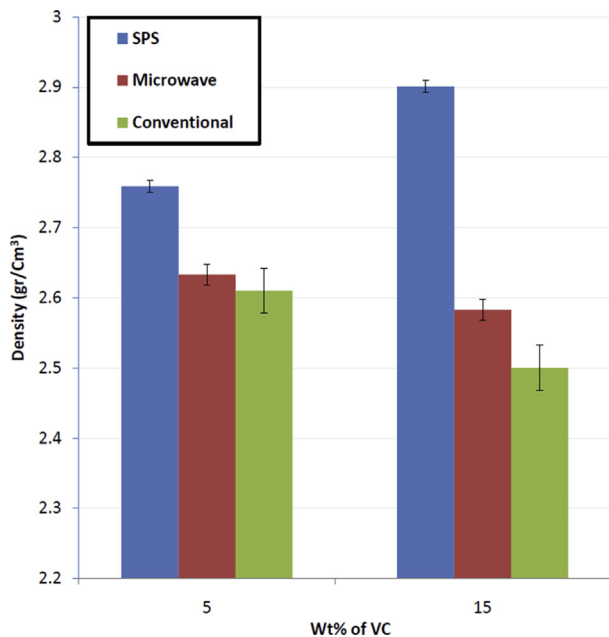
Fig. 7. Density changes vs. reinforcement content of the samples prepared with different heating methods.

Figs. 4 and 5 display the FESEM and elemental MAP analysis of Al and VC interfacial reaction areas in MW sintered Al-5wt%VC and Al-15wt% VC composites, respectively. As can be figured out from Fig. 4, the approximately partial reactions between Al and VC lead to form Al_3V intermetallic compound at the interfaces of matrix and the reinforcement. The elemental MAP analysis also confirms a limited diffusion of Al (blue colored) into the VC compound (combination of red and green colors). On the other hand, the interface of the reaction area in the MW sintered Al-15wt%VC sample shows an almost complete formation of Al_3V compound. There are also some un-reacted VC carbides remained, which indicate that the effective parameter was not enough for the complete progress of Al_3V transformation reaction. Regarding the fact that the reaction between Al and VC needs its favorable condition to occur, some parameters affect the progress of this reaction such as the sintering temperature and the reactant molar mass under a constant applied pressure. But it is worth mentioning that the reaction progress is basically related to the exact temperature of the reaction and the volume (mass/molar) fractions. Therefore, the temperatures measured by thermocouples and pyrometers might present the whole temperature of the sample only when this temperature reaches an equilibrium.

In fact, in microscopic scale, the generated heat inside the particles causes the difference between the exact and measured sintering temperatures.

Fig. 6 reveals the schematic principles of heat generation in three different sintering methods. As can be seen from Fig. 6, the conventional heating leads to an equilibrium temperature zone among all particles and soaking time can affect the reaction products and the densification regime. Also, the nature of the matrix as its wettability with the reinforcements is important in occurrence of a perfect sintering process. In the case of microwave sintering, the absorber particles play an original role on the heat generation. As it is well approved, carbide particles

usually exhibit high absorbing features due to high Tan δ. In this research, the VC particles absorb and transform the microwaves into heat (Fig. 6). Therefore, the areas having higher amounts of absorber particles can produce higher amounts of generated heat. Such a locally generated heat can create a higher exact temperature than the measured sintering temperature especially at the areas with the maximum amounts of the absorbers (VC agglomerates) [7, 10, 32]. Totally, the agglomerates in microwave sintering produce higher exact temperatures than 600 °C (measured sintering temperature) and would be followed by the progress in the formation of Al_3V. Fig. 6 also proposes the sintering mechanism in the SPS process. In the cases of conductive materials such as Al and Cu, the electrical current can pass through the specimen, while this passing is accompanied with electrical discharges known as sparks. As can be seen from Fig. 6, the preferred direction is assumed as Al–Al passing instead of VC agglomerates. Also, it is important to mention that these directions are changed by applying pressure and deformation of the samples. Perhaps lots of these directions are created/eliminated within a tiny span of time until the numerous sparks in higher local temperatures (than the measured macroscopic temperature of the die) together with the local melting at particle surfaces complete the densification of the whole sample [18, 33, 34].

Fig. 7 demonstrates the density changes versus VC content for the samples prepared with SPS, MW and conventional sintering processes. The relative density of the samples cannot be exactly calculated due to the interfacial reactions that lead to form un-known amounts of products. The density of the samples in Fig. 7 shows an increase with increasing the VC content for the SPSed samples, while for the microwave and conventionally-sintered samples, the densities decrease. The two main factors affecting the final density of the samples are: 1) the density of the composite components and 2) the presence of porosities. As mentioned before, in microwave heating the Al_3V intermetallic compound, with a lower density than VC reinforcement, is formed. Therefore, the higher formation of the interfacial products leads to a decrease in the final density of the sample with 15wt%VC. Similarly, in conventional sintering process, it seems that the VC agglomerates with high porosity concentrations, decrease the final density of the same sample. Regarding the above-mentioned factors affecting the final density, the SPSed sample with a higher content of VC shows the highest density due to the full densification behavior of the sample.

Table 1 demonstrates the mechanical properties of the samples prepared with SPS, MW and conventional sintering processes. As can be figured out from Table 1, the SPSed samples show the best mechanical properties including the bending strength and hardness. As it is expected, the full-densification behavior of the SPSed samples, which was confirmed by both FESEM images and the displacement change curves (Figs. 1 and 3), leads to the highest values of mechanical properties in the Al-15wt%VC composite. It seems that the applied pressure during the SPS process can fill up the porosities between the agglomerates. The SPSed Al-5wt%VC composite exhibits a rather uniform distribution of VC in the matrix, but the lower amount of the reinforcement results in the lower value of the bending strength and hardness, possibly due to the fewer barriers against the movements of mobile dislocations. In microwave and conventionally-prepared samples (as pressureless sintering methods), there is a decrease in the bending strength and hardness test values compared to those in SPS prepared samples. Totally, the presence of porosities as crack-initiating sites has a strong effect on the strength of the samples. In microwave sintering process, the samples with higher

Table 1

Mechanical properties of the samples prepared with SPS, MW and conventional sintering processes.

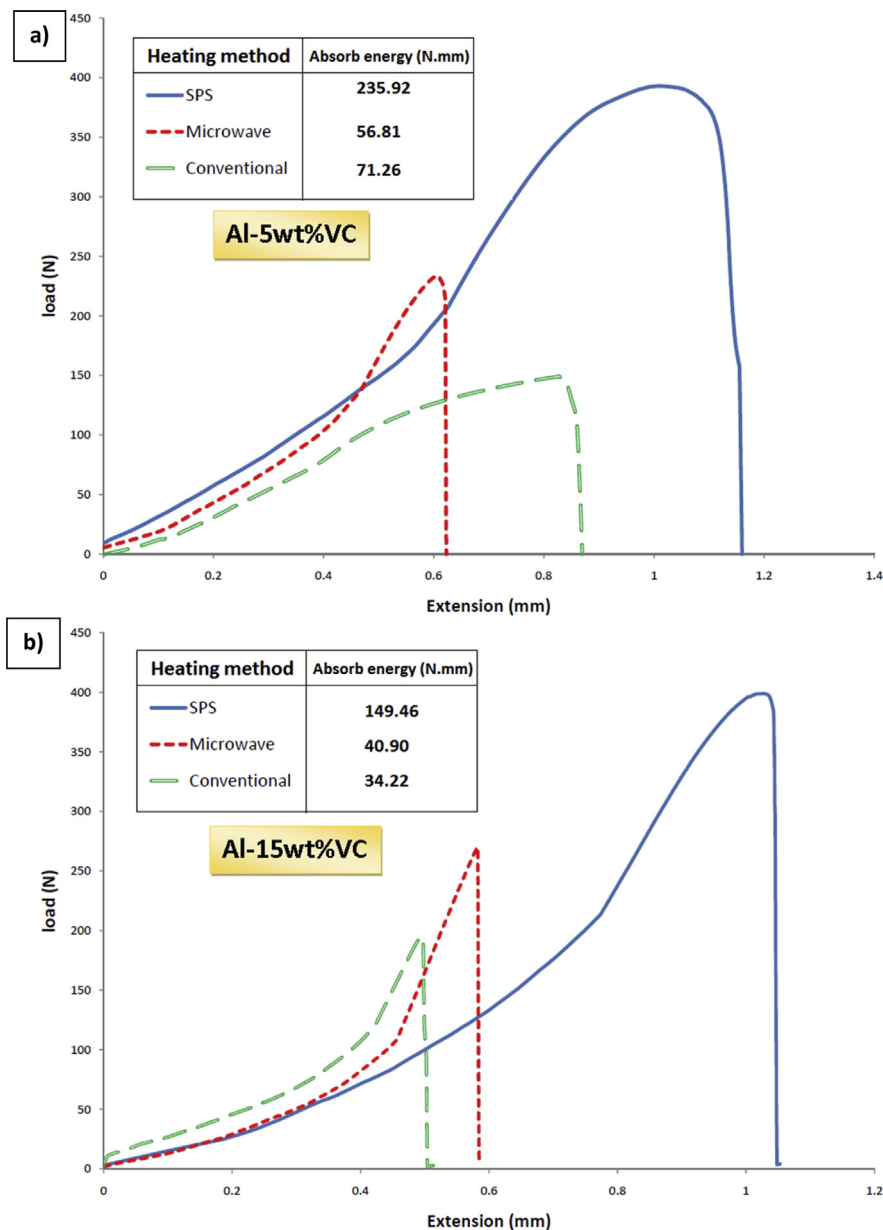| SPS		Microwave		Conventional		Properties/Sintering method
15wt%VC	5wt%VC	15wt%VC	5wt%VC	15wt%VC	5wt%VC	
275±13	243±13	132±10	110±9	75±11	103±9	Bending strength (MPa)
260±13	162±13	131±12	95±14	101±10	70±11	Hardness (Hv)

Fig. 8. Load-extension curves during the bending strength test for the SPS, microwave and conventionally-sintered Al-5wt%VC (a) and Al-15wt%VC (b) composites.

amounts of VC content as "the absorbers", form higher amounts of interfacial products that somehow interact with porosities to eliminate a fraction of them. Therefore, the lower amount of VC content in Al-5wt% VC composite leads to form lower amounts of interfacial products as discussed above, and results in lower mechanical properties compared to the sample with 15wt%VC content. Finally, the conventionally-processed Al-15wt%VC composite forms agglomerates along with inherent porosities and makes a sample with the lowest bending strength values. But, regarding the hardness test, the higher amounts of VC content result in higher hardness values in the Al-15wt%VC composite compared to the samples with 5wt%VC reinforcement particles.

Fig. 8 displays the load-extension curves during the bending strength test for all the prepared samples and also, the total absorbed energy of the samples right before fracture obtained by calculating the surface area under curves, as a criteria of the toughness [35, 36, 37]. As it is expected, the maximum fracture load and absorbed energy are reported for the SPSed Al-15wt%VC sample. On the other hand, the maximum extension is reported for the SPSed Al-5wt%VC composite. It seems that the presence of higher amount of Al in this sample with its work-softening nature

together with the microstructure free from porosities lead to such a phenomenon. In both composites, the microwave sintered samples show higher fracture load values compared to the conventionally-prepared samples. However, in the case of the absorbed energies of MW prepared samples, the higher amounts of VC particles result in higher absorbed energy values, due to the increase in the interfacial reactions. Moreover, the lowest fracture load and extension values belongs to the conventionally-prepared Al-15wt%VC composite, which is due to the harmful effect of high contents of agglomerates and porosities in the sample.

4. Conclusions

In this study, Al-VC composites have been prepared successfully via spark plasma, MW and conventional sintering processes. Investigations on the effects of different heating methods on the microstructures of the samples lead to propose a sintering mechanism based on the electrical current direction, absorber particles and the neck growth sintering process. The microwave sintering of the high-content VC particle composite

demonstrates an increase in the amount of interfacial reactions (formation of Al_3V intermetallic compound), while in the conventionally-prepared composite with the same sintering temperature (600 °C) and a higher soaking time, no interfacial reaction was observed according to the XRD and FESEM evidences. The near-full densification behavior is reported for the SPSed samples, as the pressure assisted method, and the highest mechanical property values of 275 ± 13 MPa (bending strength) and 260 ± 13 Vickers (hardness) are obtained for the composite with 15wt%VC reinforcement particles. In all the prepared samples with 5wt%VC content, a uniform distribution of the reinforcement particles in the matrix was observed. Moreover, the agglomeration phenomenon in MW sintering process proved to have a positive effect on the formation of the interfacial products and also on the mechanical properties of the composites.

Declarations

Author contribution statement

Ehsan Ghasali, Yasin Orooji: Conceived and designed the experiments; Performed the experiments; Analyzed and interpreted the data; Contributed reagents, materials, analysis tools or data; Wrote the paper.

Hadi Niknam Germib: Analyzed and interpreted the data; Wrote the paper.

Competing interest statement

The authors declare no conflict of interest.

Additional information

No additional information is available for this paper.

References

[1] S.-J.L. Kang, Sintering: Densification, Grain Growth and Microstructure, Butterworth-Heinemann, 2004.

[2] E. Ghasali, A. Fazili, M. Alizadeh, K. Shirvanimoghaddam, T. Ebadzadeh, Evaluation of microstructure and mechanical properties of Al-TiC metal matrix composite prepared by conventional, microwave and spark plasma sintering methods, Materials 10 (2017) 1255.

[3] E. Ghasali, H. Nouranian, A. Rahbari, H. Majidian, M. Alizadeh, T. Ebadzadeh, Low temperature sintering of aluminum-zircon metal matrix composite prepared by spark plasma sintering, Mater. Res. 19 (2016) 1189–1192.

[4] H. Majidian, E. Ghasali, T. Ebadzadeh, M. Razavi, Effect of heating method on microstructure and mechanical properties of zircon reinforced aluminum composites, Mater. Res. 19 (2016) 1443–1448.

[5] E. Ghasali, M. Alizadeh, M. Niazmand, T. Ebadzadeh, Fabrication of magnesium-boron carbide metal matrix composite by powder metallurgy route: comparison between microwave and spark plasma sintering, J. Alloy. Comp. 697 (2017) 200–207.

[6] E. Ghasali, R. Yazdani-rad, A. Rahbari, T. Ebadzadeh, Microwave sintering of aluminum-ZrB2 composite: focusing on microstructure and mechanical properties, Mater. Res. 19 (2016) 765–769.

[7] P. Matli, R. Shakoor, A. Amer Mohamed, M. Gupta, Microwave rapid sintering of Al-metal matrix composites: a review on the effect of reinforcements, microstructure and mechanical properties, Metals 6 (2016) 143.

[8] F. Shojai, T.A. Mäntylä, Effect of sintering temperature and holding time on the properties of 3Y-ZrO2 microfiltration membranes, J. Mater. Sci. 36 (2001) 3437–3446.

[9] A. Leriche, E. Savary, A. Thuault, J. Hornez, M. Descamps, S. Marinel, Comparison of conventional and microwave sintering of bioceramics, in: Adv. Process. Manuf. Technol. Nanostructured Multifunct. Mater. A Collect. Pap. Present. 38th Int. Conf.

[10] C. Padmavathi, D. Agarwal, A. Upadhyaya, Microwave Sintering of Aluminium Alloys, 2015.

[11] E. Ghasali, R. Yazdani-rad, K. Asadian, T. Ebadzadeh, Production of Al-SiC-TiC hybrid composites using pure and 1056 aluminum powders prepared through microwave and conventional heating methods, J. Alloy. Comp. 690 (2017) 512–518.

[12] C.T. Hammann, High Pressure Spark Plasma Sintering Followed by Electric Annealing of AlCoCrFeNi High Entropy Alloy, 2016.

[13] D. Zhang, Z. Fu, R. Yuan, J. Guo, Spark plasma sintering: a promising new technique and its mechanism, in: Multiphased Ceram. Mater., Springer, 2004, pp. 65–75.

[14] E. Ghasali, K. Shirvanimoghaddam, A.H. Pakseresht, M. Alizadeh, T. Ebadzadeh, Evaluation of microstructure and mechanical properties of Al-TaC composites prepared by spark plasma sintering process, J. Alloy. Comp. 705 (2017) 283–289.

[15] N. Al-Aqeeli, Processing of CNTs reinforced Al-based nanocomposites using different consolidation techniques, J. Nanomater. 2013 (2013) 125.

[16] C. Hu, F. Li, D. Qu, Q. Wang, R. Xie, H. Zhang, S. Peng, Y. Bao, Y. Zhou, Developments in hot pressing (HP) and hot isostatic pressing (HIP) of ceramic matrix composites, Adv. Ceram. Matrix Compos. (2014) 164–189.

[17] E. Ghasali, A.H. Pakseresht, M. Agheli, A.H. Marzbanpour, T. Ebadzadeh, WC-Co particles reinforced aluminum matrix by conventional and microwave sintering, Mater. Res. 18 (2015) 1197–1202.

[18] K.K. Chawla, Metal Matrix Composites, Wiley Online Library, 2006.

[19] B.V. Ramnath, C. Elanchezhian, R.M. Annamalai, S. Aravind, T.S.A. Atreya, V. Vignesh, C. Subramanian, Aluminium metal matrix composites–a review, Rev. Adv. Mater. Sci. 38 (2014).

[20] S.T. Mavhungu, E.T. Akinlabi, M.A. Onitiri, F.M. Varachia, Aluminum matrix composites for industrial use: advances and trends, Procedia Manuf 7 (2016) 178–182.

[21] R. Casati, Aluminum Matrix Composites Reinforced with Alumina Nanoparticles, Springer, 2016.

[22] O.S. Salih, H. Ou, W. Sun, D.G. McCartney, A review of friction stir welding of aluminium matrix composites, Mater. Des. 86 (2015) 61–71.

[23] M.O. Bodunrin, K.K. Alaneme, L.H. Chown, Aluminium matrix hybrid composites: a review of reinforcement philosophies; mechanical, corrosion and tribological characteristics, J. Mater. Res. Technol. 4 (2015) 434–445.

[24] R.S. Rana, R. Purohit, S. Das, Review of recent studies in Al matrix composites, Int. J. Sci. Eng. Res. 3 (2012) 1–16.

[25] A. V Muley, S. Aravindan, I.P. Singh, Nano and hybrid aluminum based metal matrix composites: an overview, Manuf. Rev. 2 (2015) 15.

[26] X. Qu, L. Zhang, W.U. Mao, S. Ren, Review of metal matrix composites with high thermal conductivity for thermal management applications, Prog. Nat. Sci. Mater. Int. 21 (2011) 189–197.

[27] E. Ghasali, A.H. Pakseresht, M. Alizadeh, K. Shirvanimoghaddam, T. Ebadzadeh, Vanadium carbide reinforced aluminum matrix composite prepared by conventional, microwave and spark plasma sintering, J. Alloy. Comp. 688 (2016) 527–533.

[28] E. Ghasali, T. Ebadzadeh, M. Alizadeh, M. Razavi, Unexpected SiC nanowires growth during spark plasma sintering of WC-10Si: a comparative study on phase formation and microstructure properties against WC-10Co cermet, J. Alloy. Comp. 786 (2019) 938–952.

[29] E. Ghasali, A. Pakseresht, A. Rahbari, H. Eslami-shahed, M. Alizadeh, T. Ebadzadeh, Mechanical properties and microstructure characterization of spark plasma and conventional sintering of Al–SiC–TiC composites, J. Alloy. Comp. 666 (2016) 366–371.

[30] E. Ghasali, M. Alizadeh, T. Ebadzadeh, Mechanical and microstructure comparison between microwave and spark plasma sintering of Al–B 4 C composite, J. Alloy. Comp. 655 (2016) 93–98.

[31] E. Ghasali, M. Alizadeh, T. Ebadzadeh, A.H. Pakseresht, A. Rahbari, Investigation on microstructural and mechanical properties of B4C-aluminum matrix composites prepared by microwave sintering, J. Mater. Res. Technol. 4 (2015) 411–415.

[32] M. Oghbaei, O. Mirzaee, Microwave versus conventional sintering: a review of fundamentals, advantages and applications, J. Alloy. Comp. 494 (2010) 175–189.

[33] R.S. Dobedoe, G.D. West, M.H. Lewis, Spark plasma sintering of ceramics: understanding temperature distribution enables more realistic comparison with conventional processing, Adv. Appl. Ceram. 104 (2005) 110–116.

[34] O. Guillon, J. Gonzalez-Julian, B. Dargatz, T. Kessel, G. Schierning, J. Räthel, M. Herrmann, Field-assisted sintering technology/spark plasma sintering: mechanisms, materials, and technology developments, Adv. Eng. Mater. 16 (2014) 830–849.

[35] E. Ghasali, Y. Palizdar, A. Jam, H. Rajaei, T. Ebadzadeh, Effect of Al and Mo addition on phase formation, mechanical and microstructure properties of spark plasma sintered iron alloy, Mater. Today Commun. 13 (2017) 221–231.

[36] E. Ghasali, T. Ebadzadeh, M. Alizadeh, M. Razavi, Mechanical and microstructural properties of WC-based cermets: a comparative study on the effect of Ni and Mo binder phases, Ceram. Int. 44 (2018) 2283–2291.

[37] E. Ghasali, M. Alizadeh, A.H. Pakseresht, T. Ebadzadeh, Preparation of silicon carbide/carbon fiber composites through high-temperature spark plasma sintering, J. Asian Ceram. Soc. 5 (2017).